Single cell RNA-seq analysis reveals compartment-specific heterogeneity and plasticity of microglia

Junying Zheng[1*], Wenjuan Ru[1*], Jay R Adolacion[2*], Michael S Spurgat[1], Xin Liu[1], Subo Yuan[1], Rommel X Liang[3], Jianli Dong[3], Andrew Potter[4], Steven S Potter[4], Navin Varadarajan[2], Shao-Jun Tang[1†]

[1]Department of Neuroscience, Cell Biology, & Anatomy, The University of Texas Medical Branch, Galveston, TX; [2] Department of Chemical & Biomolecular Engineering, University of Houston, Houston, TX; [3] Department of Pathology, The University of Texas Medical Branch, Galveston, TX;
[4] Division of Developmental Biology, Children's Hospital Medical Center, Cincinnati, OH

[*] These authors contributed equally to this work.

[†] Corresponding author: Shao-Jun Tang, Department of Neuroscience, Cell Biology, & Anatomy, The University of Texas Medical Branch, 301 University Blvd, Galveston, TX, shtang@UTMB.EDU

Abstract

Microglia are heterogeneous and ubiquitous CNS-resident macrophages that maintain homeostasis of neural tissues and protect them from pathogen attacks. Yet, their differentiation in different compartments remains elusive. We performed single cell RNA-seq (scRNA-seq) analysis to compare the transcriptomes of 32760 microglia in adult mouse (C57/Bl) brains and spinal cords to identify microglial subtypes in these CNS compartments. Cortical microglia from 2-month mice consisted of a predominant population of the homeostatic subtype (HOM-M) and a small population (4%) of the inflammatory subtype (IFLAM-M), while spinal microglia consisted of 55% HOM-M and 45% IFLAM-M subtype. Comparison of cortical and spinal microglia at 2, 4 and 8 months revealed consistently a higher composition of the IFLAM-M subtype in the spinal cord. At 8-month, cortical microglia differentiated a small new subtype with interferon response phenotypes (INF-M), while spinal microglia polarized toward a proinflammatory phenotype, as indicated by the increase of microglia expressing IL-1β. To further characterize the differential plasticity of cortical and spinal microglial heterogeneity, we determined the microglial transcriptomes from HIV-1 gp120 transgenic (Tg) mice, a model of HIV-associated neurological disorders. Compared with wilt-type (Wt) cortical microglia, the gp120tg cortical microglia had three new subtypes, with signatures of interferon I response (INF-M), cell proliferation (PLF-M), and myelination or demyelination (MYE-M) respectively; while INF-M and PLF-M subtypes presented at all ages, the MYE-M only at 4-month. In contrast, only the INF-M subtype was observed in the spinal microglia from 2- and 4-month gp120tg mice. Bioinformatic analysis of regulated molecular pathways of individual microglial subtypes indicated that gp120 more severely impaired the biological function of microglia in cortices than in the spinal cord. The results collectively reveal differential heterogeneity and plasticity of cortical and spinal microglia, and suggest functional differentiation of microglia in different CNS compartments.

Introduction

The CNS-resident macrophages, microglia, play critical roles in CNS development, homeostasis and inflammation. During development, microglia participate in neural circuit formation by regulating specific processes such as axon outgrowth and synapse maturation and pruning[1,2]. In adults, microglia actively survey the microenvironment to maintain homeostasis[3]. In response to infection or injury, microglia are activated to remove pathogens, damaged cells and dysfunctional synapse, and facilitate tissue repair [4].

The diverse functionality likely arises from different microglial subtypes with distinct morphologies and biological activities. For instance, non-phagocytic activated microglia appear bushy with short thick branches, undergo rapid proliferation, and secrete pro-inflammatory signalling molecules[5], whereas phagocytic activated microglia show an ameboid shape, and can travel to injury sites to engulf cell debris[3,5]. From the perspective of inflammation, activated microglia are classically categorized into pro-inflammatory M1 and anti-inflammatory M2 subtypes. M1 microglia produce pro-inflammatory mediators such as TNF-a, IL-1β, and NO[6,7], while M2 microglia express anti-inflammatory mediators[8]. The biological basis of microglial heterogeneity is still poorly understood.

Single cell RNA-seq (scRNA-seq) provides powerful means to characterize microglial heterogeneity. Transcriptomic data generated from this approach revealed novel microglial subtypes[9,10]. Microglia appear more heterogeneous during early development, compared with adult stages[10,11]. Yet, microglia in adult brains are still plastic and can adapt to different phenotypes in response to pathogenic insults, including subtypes beyond the M1 and M2 categories. At least four activated microglial subtypes with hallmarks of inflammation, proliferation, interferon response, and demyelination respectively have been identified in mouse models of aging and neurodegenerative diseases[9–14].

Emerging scRNA-seq evidence suggests spatial and temporal heterogeneity of microglia in the brain[3]. These findings indicate regional- and age-dependent plasticity of microglia. However, the mechanism and biological significance of the spatial- and temporal-regulated microglial heterogeneity are unclear.

In this study, we performed scRNA-seq analysis on unsorted cells dissociated from brain cortices and spinal cords to compare microglial heterogeneity in the cortex and the spinal cord of adult mice. We found that in Wt mice both cortical and spinal microglia were consisted of the homeostatic and inflammatory subtypes although with differential proportions, and that cortical and spinal microglia respond differently to age progression. We further demonstrated differential plasticity of microglia in cortices and spinal cords in a mouse model of HIV-associated neurological complications. The findings suggest a region-specific mechanism in controlling the expression of microglial phenotypes and the differentiation of microglial functions in different CNS compartments.

Results

Microglial heterogeneity in the brain cortex and the spinal cord from 2-month wild type adult mice.

To understand the spatial heterogeneity of microglia in the CNS in an unbiased manner, we performed droplet-based scRNA-seq[15] on cells dissociated from Wt adult mouse (2-month) brain cortices and spinal cords (Sup. Fig. 1a). We adapted and optimized a density gradient cell separation protocol[16] to minimize cell death from dissociation processes and collected the fractions enriched with microglia for the downstream scRNA-seq processing. Cells dissociated from two cortices and two whole spinal cords were pooled respectively. Total of 19960 unsorted cells from cortices (10000) and spinal cords (9961) were sequenced to a depth of ~30,000 raw reads per cell. Cells with over representation of mitochondrial genes (>10%) or low number of detected gene (<300/cell) were filtered out (Sup. Fig. 1b). 5211 cells from the cortex (52 % of cortical cells) and 3780 cells from the spinal cords (38% of spinal cells) passed quality control for downstream analysis. We performed t-distributed stochastic neighbor embedding (t-SNE) cluster analysis (Seurat v2.21) on cortical or spinal cells. The resolution 0.6 was used for all t-SNE analysis in this study. The t-SNE analysis identified 14 clusters (Fig. 1a; Sup. Fig. 1c; Sup. Fig. 1d), and individual clusters displayed characteristic expression of specific sets of genes (Sup. Fig. 1e) that defined the cell types of each cluster (Fig. 1a). We found all major types of cells in the clusters of cortical cells,

including neurons, microglia, astrocytes and oligodendrocytes, with neurons markedly under represented (Fig. 1a). Similar cell types were detected in the spinal clusters, except that few neurons were present (Fig. 1b). These data indicate microglia were the predominant clusters on the t-SNE plots from both the cortical and spinal cells, with few neurons due to the fraction we collected (Fig. 1a; Fig. 1b).

We used multiple gene markers, including Cx3cr1, P2ry12 and Tmem119, to identify microglia (Fig.1a; Fig. 1b; Sup. Fig.1e). Three microglial clusters were identified from the cortex on the t-SNE plot (Fig. 1a), while two microglial clusters from the spinal cord (Fig. 1b). These observations indicated a differentiation between cortical and spinal microglia. To further visualize this difference, we performed Seurat Canonical Correlation Analysis (CCA) analysis on pooled cortical and spinal microglia. As shown in Fig. 1c, cortical and spinal microglia only partially overlapped, showing the differential transcriptomic expression of the two microglial populations.

To gain more insights into the biological basis of the differences between cortical and spinal microglia, we sought to determine the microglial subtypes of individual clusters revealed by t-SNE analysis, based on their uniquely expressed genes. We found that two major microglial clusters in the cortical t-SNE plot (clusters 0 and 2 in Fig. 1a) with high expression of homeostatic genes (e.g. Cx3cr1, Tmem119, P2ry12, Csf1r)[11], and thus named them as homeostatic microglia (HOM-M) (Fig. 1d; Fig. 1d). The HOM-M subtype constituted 94% of cortical microglia. As shown by the clusters on the t-SNE plot (Fig. 1a) and gene expression heatmap (Fig. 1d), the cortical HOM-M was consisted of two computationally polarized two groups, HOM-M1 and HOM-M2. HOM-M1 has slightly lower expression of genes coding ribosomal protein (e.g. Rps11, Rps21, Rpl26) and Rgs10, the gene coding a member of regulator of G protein signaling family[17] (Fig. 2a). HOM-M microglia were enriched with the expression of genes in various molecular pathways that are implicated in maintaining homeostatic functions such as P2ry12, consistent with a role of HOM-M microglia in damage-sensing[18]. We also found HOM-M in the spinal microglia, corresponding to cluster 0 on the spinal t-SNE plot (Fig. 1b). The spinal HOM-M constituted 55% of the microglial population. In contrast to the polarization of cortical HOM-M into two groups (HOM-M1 and HOM-M2), the spinal HOM-M microglia were not further polarized within the subtype into different clusters (Fig. 1b; Fig. 1d).

Another microglial subtype was identified by their uniquely expression of genes regulating immune response (e.g. Il1a, Il1b, Ccl3, Ccl4), and thus named inflammatory microglia (IFLAM-M). This subtype corresponded to cluster 9 in the cortical t-SNE plot (Fig. 1a). Microglia enriched with cytokine and chemokine genes (e.g. Il1b, Ccl2, Ccl4) were previously found from scRNA-seq analysis of human and mouse brains[11,14]. They were described as inflammatory microglia[14] or preactivated microglia[11]. In addition to sharing similar profiles of inflammatory mediators, IFLAM-M, the inflammatory microglia[14] and preactivated microglia[11] all expressed immediate early genes (IGEs) such as c-fos, Egr1 and Atf3, indicating that they are a similar microglial subtype. The IFLAM-M microglia were enriched with the expression of genes involved in cytokines such as Il1b (Fig. 1e), indicating the biological function of this subtype of microglia in mediating proinflammation. Cortical microglia from 2-month mice only had a small population (4%) of IFLAM-M (Fig. 1a; Fig. 1d). In contrast, IFLAM-M constituted 45% of spinal microglia (cluster 2 in Fig. 1b; Fig. 1d). The different sizes of cortical and spinal IFLAM-M populations were confirmed by the feature plots of microglial marker genes (Cx3cr1, P2ry12) and IFLAM-M enriched genes (Sup. Fig. 2), as well as by RNA in situ hybridization (RNAscope) of Cd83 (Fig. 1f; Fig.1g), one of the most consistent marker of IFLAM-M (Fig. 1d).

The temporal differentiation of cortical and spinal microglial plasticity

The observations of differentiation of cortical but not spinal HOM-M and the drastic difference in population sizes of HOM-M and IFLAM-M in the cortex and the spinal cord suggest differential heterogeneity of cortical and spinal microglia in the 2-month mice. Next,

we sought to determine if the cortical and spinal microglia showed different plasticity. To this end, we compared transcriptomes of cortical and spinal microglia at different animal ages (2-, 4- and 8-month). The remarkable difference in population sizes of HOM-M and IFLAM-M in the cortex and spinal cord revealed at two months of age sustained at 4-, and 8-months (Fig.2a; Fig. 2b; Sup. Fig. 3). HOM-M were the majority cortical microglia, with 96%, 92% and 98% at 2-, 4 and 8-months respectively, whereas the cortical IFLAM-M only appeared at 2 and 4 months, with 4% and 8% respectively.

Same as the 2-month, cortical HOM-M were polarized into HOM-M1 and HOM-M2 at 4- and 8-months (Fig. 2a). Compared to HOM-M2, HOM-M1 expressed relevant lower level of genes coding ribosomal protein and regulator of G protein signaling (e.g. Rps11, Rps21, Rpl26, Rgs10). The functional difference between these two clusters is unknown. However, the recent findings of microglial RGS10 as an anti-inflammatory and neuroprotective mediator[19] suggest HOM-M1 and HOM-M2 may play different roles in CNS inflammation and homeostasis maintenance. In contrast to the cortical microglia, no polarization of spinal HOM-M was observed at all ages (Fig. 2b).

The cortical IFLAM-M comprised 4% and 8% of total cortical microglia at 2- and 4-months respectively (Fig.2a). These microglia expressed inflammatory cytokines (e.g. Il1, Ccl3, CCL4). At 8month, the cortical IFLAM-M was not detected. Unlike the small cortical IFLAM-M clusters, the spinal IFLAM-M comprised a large population (41% ~ 54%) of spinal microglia. Spinal IFLAM-M displayed evident alteration during aging. At 2- and 8-month, they formed one cluster (Fig. 2b). While at 4-month, IFLAM-M were segregated into two clusters, IFLAM-M1 and IFLAM-M2 (Fig. 2b). IFLAM-M1 expressed genes (e.g. Atf3, Zfp36, Jun, Ccl4, Ccl3, Tnf, Il1α) that regulate acute response and inflammation[20,21], while IFLAM-M2 expressed genes (e.g. Cd14, Gpr84, C5ar1, C3ar1) that module microglia activation [22,23] and complement response [24]. In addition, we found that the percentage of microglia expressing Cd83, Cd14 and Il1b was increased in the spinal cord at 8-month (Fig. 2c) but not in the brain cortex, suggesting a polarization of spinal microglia toward a pro-inflammatory phenotype at this stage [22,25].

At 8month, a small cortical microglial cluster (2% of cortical microglia) with the signature of interferon-response genes (e.g. Ifit2, Ifit3, and Ifi204) emerged (Fig. 2a), and was named as interferon response microglia (INF-M). Interferon-related microglia were also found in an Alzheimer's disease mouse model[13] and aged mouse brains[14]. INF-M and the previously identified interferon-related microglia[26] shared the expression of multiple interferon-stimulated genes, although fewer members were identified in INF-M. IFN-M was not detected in spinal microglia at the same stage (Fig. 2b).

A small (3%) spinal-specific microglial cluster appeared at 8-month, with a signature expression of a set of genes implicated in proliferation and cell cycle control (e.g. Mki67, Top2a) (Fig. 2b). We named this cluster as proliferation related microglia (PLF-M). Microglia expressing proliferative genes were identified in the developing white matter as proliferative-region-associated microglia (PAM)[10]. However, we did not detect in PLF-M the expression of phagocytosis-related genes, which was a signature of PAM[10]. PLF-M was not detected in the cortical microglia.

Cortical and spinal microglial heterogeneity in HIV-1 gp120 Transgenic mice at two months of age

The results described above revealed microglial cortical- and spinal-specific heterogeneity, and the significance of this compartment-specific heterogeneity is suggested by its age-related differential plasticity. Because microglia are CNS resident immune cells, we sought to further confirm the biological relevance of the compartment-specific microglial heterogeneity by determining their response to pathogenic challenges. To this end, we used the HIV-1 gp120 transgenic (Tg) mouse , which expresses secreted gp120 in astrocytes and simulates HIV-associated neurological pathologies[27]. We found that microglial heterogeneity was increased both in the cortex and the spinal cord of the Tg mice at two months of age

(Fig. 3a; Fig. 3b), compared with the age-matched Wt animals (Fig. 1a; Fig. 1b). Five microglial clusters were identified in the 2-month Tg cortex (Fig. 3a). Based on the transcriptomic signature, these clusters included the HOM-M (cluster 0 and 1), IFLAM-M (cluster 3), IFN-M (cluster 8) and PLF-M (cluster 7) (Fig. 3a; Fig. 3c). Compared with that in age-matched Wt mice, two new subtypes PLF-M and INF-M were induced in the transgenic mice (Fig. 3d), with each constituting ~4% of total cortical microglia.

Compared with cortical microglia, spinal microglia responded differently in the Tg mice at 2-months. Three spinal microglial subtypes were identified (Fig. 3b) including the HOM-M (cluster 1 and 2), IFLAM-M (cluster 0) and IFN-M (cluster 12) (Fig. 3b&3c). While the IFN-M subtype, which was not detected in WT cortical and spinal microglia at 2-months (Fig.1), was induced in both cortical and spinal microglial populations in the Tg mice at the same stage (Fig. 3d). The PLF-M subtype was only induced in the Tg cortical microglia but not in the spinal counterpart (Fig. 3d).

Age-gp120 interaction differentially promoted cortical and spinal microglial heterogeneity

The data described above revealed differential plasticity of cortical and spinal microglial heterogeneity in response to age progression or gp120-induced pathogenesis. Next, we sought to test the interactive effect of age progression and gp120 on the expression of heterogeneity plasticity of cortical and spinal microglia. To this end, we determined the temporal profiles of cortical and spinal microglial subtypes at different ages (2-, 4-, and 8-month) of the Tg mice. We observed that cortical microglia displayed distinct but overlapping subtypes as age progression. As at 2-month, cortical microglial heterogeneity increased both at 4-month and 8-month in the Tg mice, compared with the cortical microglial subtypes from the age-matched WT mice (Fig.4a). Five cortical microglial subtypes were identified at 4-month Tg mice; they included HOM-M, IFLAM-M, INF-M and PLF-M, which were detected in the 2-month cortical microglia and a new subtype not detected in the 2-month cortical microglia (Fig. 4a; Fig. 4b). This new subtype comprised 11% of total cortical microglia, and was named as MYE-M because it had the signature expression of genes that promote myelination and remyelination (e.g. Lpl, Cst7, Igf1, Spp1, Fabp5, Itgax)[28–30]. Compared to the age-matched Wt, the population of IFLAM-M increased in the 2 and 4-month Tg cortices (Fig. 4b; Fig. 7b). The 8-month Tg cortical microglia contained overlapping clusters with 2- and 4-month Tg cortices except the MYE-M (Fig. 4a; Fig. 4b). MYE-M appeared in the 4-month cortex was not detected in the 8-month Tg cortex (Fig. 4a; Fig. 4b). In contrast, the INF-M and PLF-M remained (Fig. 4b). The population of INF-M gradually increased from 2- to 8-month in the Tg corices and reached the highest at 8-month which covering 11% of the total cortical microglial population (Fig. 4b; Fig. 7b). Population of PLF-M did not show significant changes in the Tg cortices along age progressing (Fig. 4b; Fig. 7b).

In contrast to the differentiation of multiple new cortical microglial subtypes in the Tg mice at 2-, 4- and 8-month compared with the WT cortical microglia as described above, the spinal microglia in the Tg mice showed few new subtypes compared with their age-matched WT counterparts. We only observed the increase of microglial heterogeneity in the 2- and 4-month transgenic mice, with the appearance of INF-M (Fig.5a; Fig. 5b) that constituted ~2% of the total spinal microglia population. The INF-M was not detected in the 8-month Tg spinal cord of Wt or Tg mice (Fig. 5c). In addition, the PLF-M observed in the Wt spinal cord at 8-month was not detected in the 8-month Tg spinal cord (Fig. 5c). As in 4-month Wt spinal microglia, the IFLAM-M in Tg spinal microglia at the correspondent stage also differentiated into IFLAM-M1 and IFLAM-M2 groups (Fig. 5b).

Differential biological activity of cortical and spinal microglial subtypes in the gp120 transgenic mice

The above data revealed the differential plasticity of cortical and spinal microglial heterogeneity in the HIV-1 gp120 transgenic mouse. We next sought to investigate if the biological functions of the same microglial subtype in the cortex and the spinal cord were differentiated in the cortex and the spinal cord of the transgenic mice. To this end, we sought to compare the activity of the cannonical pathways of cortical and spinal microglial subtypes in the WT and gp120 transgenic mice. Lists of up-regulated genes with the adjust p-value (<0.05) for individual microglial clusters (**Supplementary Table 1 and 2**) from 2-, 4-, 8-month Wt and Tg cortices and spinal cords were input into IPA to evaluate the change of individual biological pathways (e.g. immune response and nervous signalling pathways). We found many cannonical pathways in the same subtype of the cortical and spinal microglia were differentially regulated in the Tg mice. For instance, some selected cannonical pathways were evidently activated in both cortical and spinal HOM-M subtypes in WT mice, especially at 2- and 4- months (Fig. 7a, 7c). However, these pathways, except the neuroinflammation signalling, were severely attenuated in the cortical HOM-M of the transgenic mice across all ages (Fig. 7b). In the spinal cords, however, the attenuation of these pathways seemed to occur, but with a less degree compared with their cortical counterparts.

Discussion

In this study, we compared microglia from the cortices and spinal cords using scRNA-seq approaches and characterized microglial subtypes in these CNS compartments based on clustering analysis. Notwithstanding the intrinsic technical caveats associated with scRNA-seq, the multi-way comparisons enabled by including samples from different tissues (cortices and spinal cords), different ages (2-, 4- and 8-month) and different mouse lines (Wt and gp120 Tg) allowed us to evaluate the consistency among the data sets. Our results reveal an overlapping but distinct microglial populations in the cortex and the spinal cord (Fig. 7a; Fig. 7b). The differential heterogeneity is further shown by the differences in their plasticity under two neurophysiological conditions relevant to the biological function of microglia - life span progression and pathogen exposure. The findings indicate that microglia in the cortical and spinal compartments are adapted to the local environments to fulfil their unique biological functions, by differentiating distinct subtypes and/or expressing differential plasticity of the same subtypes.

Cortical- and spinal-specific microglial heterogeneity

We found that microglia in the cortex and the spinal cord in 2- and 4-month WT mice were consisted of two subtypes, HOM-M and IFLAM-M. However, the proportions between HOM-M and IFLAM were dramatically different in the cortex and the spinal cord. IFLAM-M comprised only a small portion (4-8%) of the cortical microglia, while in the spinal cord about half of microglia were IFLAM-M (Fig. 8b). Because IFLAM-M express inflammatory genes and likely play critical role in inflammatory response, these observations indicate that the cortex may have a more limited capacity in microglia-mediated inflammatory response. In contrast, the large and more active population of the spinal IFLAM-M microglia suggest an increased capacity of microglia-mediated inflammatory response of the spinal cord. The plasticity of spinal microglia was also suggested by the observation the spinal-specific plastic changes of the IFLAM-M during age progression. While spinal IFLAM-M were detected as one cluster at 2-month, then differentiated into IFLAM-M1 and IFLAM-2 at 4-month, and returned to one cluster at 8-month (Fig. 2b). IFLAM-M1 expressed multiple signature genes of the classic M1 microglia (e.g. Tnf, Il1a, Il1b), and IFLAM-M2 expressed genes regulating cell activation and complementary response (e.g. Cd14, C5ar1, C3ar1).

In the cortex of WT mice, the IFLAM-M subset of microglia disappeared at 8-month (Fig. 7b). Instead, a small cluster of IFN-M microglia was identified at this stage. INF-M microglia were of characteriscs with interferon-response genes, which are implicated in age-related

modulation of cognitive function[29]. Given the reported aging-induced interferon-related microglia[13,14], the observation of INF-M at 8-month may suggest interferon-related microglial activation during aging. It is unclear if there is a causal relationship between the disappearance of IFLAM-M and the appearance of INF-M in the 8-month cortex.

In the spinal cord at this stage, however, IFN-M was not observed (Fig. 8b). Instead, a small cluster of PLF-M microglia appeared, constituting 3% of spinal microglia (Fig. 8b). Because PLF-M microglia expressed genes regulating cell cycle and proliferation and were not observed in the cortex of WT mice at this stage, the appearance of spinal PLF-M indicated the occurrence of spinal-specific microglial proliferation during this age.

Together, the temporal comparative scRNA analysis of cortical and spinal microglia of WT mice reveals that microglia in these two CNS compartments have distinct heterogeneity and age-related plasticity. These findings suggest compartment-specific differentiation of the biological function of microglia to maintain local homeostatic function of the CNS.

Cortical- and spinal-specific plasticity of microglial heterogeneity in the HIV-1 gp120 transgenic mice

Temporal comparative scRNA analysis revealed marked differences of microglial heterogeneity in the cortex and the spinal cord of the gp120 transgenic mice (Fig. 7a; Fig. 7b). Compared to their Wt counterparts at different stages, in addition to the HOM-M and IFLAM-M subtypes, cortical microglia in the Tg mice formed three new subtypes, including INF-M, MYE-M, and PLF-M, while spinal microglia from transgenic mice only differentiated one new subtype, INF-M (Fig. 7a; Fig. 7b). PLF-M and MYE-M were cortical-specific in the transgenic mice.

Although INF-M was shared by both the cortical and the spinal microglia, it showed different temporal profiles in these compartments. Cortical IFN-M were present at all three time points, with increasing in its proportions as age progression (Fig. 7b). On the other hand, spinal INF-M appeared at both 2- and 4-month with a steady small proportion but disappeared at 8-month (Fig. 7b). As type I interferon-induced reactive microglia were implicated in engulfing neuronal and synaptic elements[33], the increase of the cortical INF-M population as age progressing may help clean damaged neural cells or debris induced by gp120. Type I interferon in spinal cords is implicated in pain suppression[34]. It would be of interest for future studies to determine if INF-M contributes to the pathogenesis in the spinal pain neural circuits induced by HIV-1 neurotoxins.

PLF-M was a cortical-specific microglial subtype that presented at all stages in the transgenic mice but absented in the spinal cord. The presence of PLF-M indicated that cortical microglia were re-entering cell cycles and proliferating in the transgenic mice. In contrast, the lack of PLF-M in the spinal cord suggested low proliferation of spinal microglia in the transgenic HIV model.

MYE-M was another cortical-specific subtype identified in the transgenic mice. However, unlike the PLF-M subtype, MYE-M was only detected in the 4-month Tg cortex (Fig. 7a; Fig. 7b). Signature genes of MYE-M (e.g. Lpl, Cst7, Igf1, Itgax, Lgals3, Spp1) (Fig. 8a) were also found to be expressed in microglial subtypes (e.g. DAM) in neurodegeneration models[9,11,13,14]. We compared the upregulated genes from MYE-M and DAM and found only 18 out of 138 MYE-M enriched genes overlapped with that from DAM (Fig. 8b). These overlapped genes included Cst7, Lpl, Itgax that are involved in myelinogenic processes[30] and phagocytosis[31]. Combined RNA scope in situ hybridization with immunohistochemistry confirmed the gp120-induced MYE-M in the Tg brain cortices (Fig. 8c; Fig. 8d; Fig. 8e). DAM was implicated in clearance of damaged neurons associated with Alzheimer's disease[9], and it is tempting to speculate a similar role of MYE-M. However, the large portion of non-

overlapped genes enriched in MYE-M and DAM suggests that these microglial subtypes are very different in their biological activities.

In summary, the findings from this study show the differential microglial heterogeneity in the mouse cortex and the spinal cord. They also demonstrate that microglia in the two CNS compartment have different plasticity in response to age advancing and gp120-induced pathogenesis. It would be interesting for future studies to elucidate the potential intrinsic and/or extrinsic mechanisms by which the compartment-associated microglial heterogeneity and plasticity origin.

Methods

Animals

Gp120 Tg mice (from Dr. Marcus Kaul, Sanford-Burnham Medical Research Institute) express HIV-1 LAV gp120 under the control of the glial fibrillary acidic protein (GFAP) promoter. All animal procedures were performed according to protocol 0904031B approved by the Institutional Animal Care and Use Committee at the University of Texas Medical Branch, and all methods were performed in accordance with the relevant guidelines and regulations.

Tissue harvesting

Mice were transcardially perfused with 1xPBS before tissue extraction. Brain cortex and the whole spinal cord were collected from the 2-, 4-, and 8-month old Wt and gp120 Tg mice respectively. For each group, tissue collected from two mice (mixed gender) were pooled together for subsequent cell dissociation.

Cell dissociation

The dissected brain cortexes and spinal cords were cut into small pieces and then digested in papain dissociation system according to the manufacturer protocol (Worthington Biochemical Corp.). Dead cells and myelin debris were removed using debris removal solution (Miltenyi Biotec.) followed by Ms colomns (Miltenyi Biotec.). Isolated cells were resuspended in Hibernated A (BrainBits, LLC). Cells with viability >90% were processed for single-cell RNASeq. All the procedures except the enzymatic digestion were keep on ice or at 4^{o}C.

Droplet-based scRNA-Seq

The droplet-based scRNA-Seq procedure was based on a protocol from Macosko et. al[15].

Processing of single-cell RNA-seq raw data

Drop-seq FASTQ files were processed using the standard pipeline (Drop-seq tools version 1.12 from McCarroll lab, http://mccarrolllab.org/wp-content/uploads/2016/03/Drop-seqAlignmentCookbookv1.2Jan2016.pdf).

Clustering analysis of scRNA-seq data

Generated read counts were analyzed in R version 3.4.4 (R Core Team 2018) via Seurat 2.2.1[35] following its standard pre-processing and clustering workflow (https://satijalab.org/seurat/pbmc3k_tutorial.html). Briefly, from the distribution of reads, the data was filtered to a minimum of 300 cells per gene and 30 genes per cell. This was followed by UMI and mitochondrial filtering and normalization prior to selecting all highly variable genes falling within a selected cutoff window for PCA clustering. Statistically significant PCs (p-value < 0.001) were used in cluster determination to produce heatmaps and t-SNE plots at a resolution of 0.6. Clusters were annotated based on the expression

level of canonical marker genes and gene expression visualized using feature maps. Seurat violin plots were consolidated using graphical packages in R.

Combination of RNAscope in situ hybridization (ISH) and immunohistochemistry
Probes for genes Cd83, Il1b, Egr1, Cst7, Lpl were purchased from Advanced Cell Diagnostics, Inc (Newark, CA). ISH including tissue pre-treatment and probes hybridization were performed following the manufactural protocol of RNAScope® Multiplex Fluorescent V2 Assay. Immediately following last wash step for ISH, the sections were washed with 1xPBS for 5min and followed by standard immunohistochemistry protocol. Rabbit anti-Iba1 antibody (1:200) was purchased from abcam (Cambridge, MA) . Images were acquired on a Zeiss LSM 880 microscope system at 60x magnification.

Canonical pathway analysis
Differential gene expression across these clusters and their cell types was carried out using a standard AUC classifier, returning only genes with adjust p-value < 0.05. These genes were imported into Ingenuity Pathway Analysis (IPA) (QIAGEN Inc.) for the downstream pathway activation analysis. A cut off p-value <0.05 and |z score| ≥2 were used to predict the significantly activated /inhibited signalling pathways.

References

1. Schafer, D. P., Lehrman, E. K. & Stevens, B. The 'quad-partite' synapse: Microglia-synapse interactions in the developing and mature CNS. *Glia* (2013) doi:10.1002/glia.22389.

2. Hoshiko, M., Arnoux, I., Avignone, E., Yamamoto, N. & Audinat, E. Deficiency of the microglial receptor CX3CR1 impairs postnatal functional development of thalamocortical synapses in the barrel cortex. *J. Neurosci.* (2012) doi:10.1523/JNEUROSCI.1167-12.2012.

3. Brioschi, S., Peng, V. & Colonna, M. Fifty Shades of Microglia. *Trends in Neurosciences* (2019) doi:10.1016/j.tins.2019.03.010.

4. Gehrmann, J., Matsumoto, Y. & Kreutzberg, G. W. Microglia: Intrinsic immuneffector cell of the brain. *Brain Research Reviews* (1995) doi:10.1016/0165-0173(94)00015-H.

5. Aloisi, F. Immune function of microglia. *Glia* (2001) doi:10.1002/glia.1106.

6. Block, M. L., Zecca, L. & Hong, J. S. Microglia-mediated neurotoxicity: Uncovering the molecular mechanisms. *Nature Reviews Neuroscience* (2007) doi:10.1038/nrn2038.

7. Le, W. D. *et al.* Microglial activation and dopaminergic cell injury: An in vitro model relevant to Parkinson's disease. *J. Neurosci.* (2001) doi:10.1523/jneurosci.21-21-08447.2001.

8. Cherry, J. D., Olschowka, J. A. & O'Banion, M. K. Neuroinflammation and M2 microglia: The good, the bad, and the inflamed. *Journal of Neuroinflammation* (2014) doi:10.1186/1742-2094-11-98.

9. Keren-Shaul, H. *et al.* A Unique Microglia Type Associated with Restricting Development of Alzheimer's Disease. *Cell* (2017) doi:10.1016/j.cell.2017.05.018.

10. Li, Q. *et al.* Developmental Heterogeneity of Microglia and Brain Myeloid Cells Revealed by Deep Single-Cell RNA Sequencing. *Neuron* (2019) doi:10.1016/j.neuron.2018.12.006.

11. Masuda, T. *et al.* Spatial and temporal heterogeneity of mouse and human microglia

at single-cell resolution. *Nature* (2019) doi:10.1038/s41586-019-0924-x.

12. Mathys, H. *et al.* Temporal Tracking of Microglia Activation in Neurodegeneration at Single-Cell Resolution. *Cell Rep.* (2017) doi:10.1016/j.celrep.2017.09.039.

13. Friedman, B. A. *et al.* Diverse Brain Myeloid Expression Profiles Reveal Distinct Microglial Activation States and Aspects of Alzheimer's Disease Not Evident in Mouse Models. *Cell Rep.* (2018) doi:10.1016/j.celrep.2017.12.066.

14. Hammond, T. R. *et al.* Single-Cell RNA Sequencing of Microglia throughout the Mouse Lifespan and in the Injured Brain Reveals Complex Cell-State Changes. *Immunity* (2019) doi:10.1016/j.immuni.2018.11.004.

15. Macosko, E. Z. *et al.* Highly parallel genome-wide expression profiling of individual cells using nanoliter droplets. *Cell* (2015) doi:10.1016/j.cell.2015.05.002.

16. Brewer, G. J. & Torricelli, J. R. Isolation and culture of adult neurons and neurospheres. *Nat. Protoc.* (2007) doi:10.1038/nprot.2007.207.

17. Hunt, T. W., Fields, T. A., Casey, P. J. & Peralta, E. G. RGS10 is a selective activator of Gα(i) GTPase activity. *Nature* (1996) doi:10.1038/383175a0.

18. Haynes, S. E. *et al.* The P2Y12 receptor regulates microglial activation by extracellular nucleotides. *Nat. Neurosci.* (2006) doi:10.1038/nn1805.

19. Lee, J. K., Chung, J., McAlpine, F. E. & Tansey, M. G. Regulator of G-protein signaling-10 negatively regulates NF-κB in microglia and neuroprotects dopaminergic neurons in hemiparkinsonian rats. *J. Neurosci.* (2011) doi:10.1523/JNEUROSCI.1002-11.2011.

20. McMahon, S. B. & Monroe, J. G. The role of early growth response gene 1 (egr-1) in regulation of the immune response. *Journal of Leukocyte Biology* (1996) doi:10.1002/jlb.60.2.159.

21. Sokol, C. L. & Luster, A. D. The chemokine system in innate immunity. *Cold Spring Harb. Perspect. Biol.* (2015) doi:10.1101/cshperspect.a016303.

22. Janova, H. *et al.* CD14 is a key organizer of microglial responses to CNS infection and injury. *Glia* (2016) doi:10.1002/glia.22955.

23. Bouchard, C., Pagé, J., Bédard, A., Tremblay, P. & Vallières, L. G protein-coupled receptor 84, a microglia-associated protein expressed in neuroinflammatory conditions. *Glia* (2007) doi:10.1002/glia.20506.

24. Freeley, S., Kemper, C. & Le Friec, G. The "ins and outs" of complement-driven immune responses. *Immunological Reviews* (2016) doi:10.1111/imr.12472.

25. Rothwell, N. J. & Luheshi, G. N. Interleukin 1 in the brain: Biology, pathology and therapeutic target. *Trends in Neurosciences* (2000) doi:10.1016/S0166-2236(00)01661-1.

26. Capuccini, B. *et al.* Transcriptomic profiling of microglia reveals signatures of cell activation and immune response, during experimental cerebral malaria. *Sci. Rep.* (2016) doi:10.1038/srep39258.

27. Yuan, S. B. *et al.* Gp120 in the pathogenesis of human immunodeficiency virus-associated pain. *Ann. Neurol.* (2014) doi:10.1002/ana.24139.

28. Ma, J. *et al.* Microglial cystatin F expression is a sensitive indicator for ongoing demyelination with concurrent remyelination. *J. Neurosci. Res.* (2011) doi:10.1002/jnr.22567.

29. Bruce, K. D. *et al.* Lipoprotein lipase is a feature of alternatively-activated microglia and may facilitate lipid uptake in the CNS during demyelination. *Front. Mol. Neurosci.* (2018) doi:10.3389/fnmol.2018.00057.

30. Nomura, K., Vilalta, A., Allendorf, D. H., Hornik, T. C. & Brown, G. C. Activated Microglia Desialylate and Phagocytose Cells via Neuraminidase, Galectin-3, and Mer Tyrosine Kinase. *J. Immunol.* (2017) doi:10.4049/jimmunol.1502532.

31. Baruch, K. *et al.* Aging-induced type I interferon response at the choroid plexus negatively affects brain function. *Science (80-.).* (2014) doi:10.1126/science.1252945.

32. Wlodarczyk, A. *et al.* A novel microglial subset plays a key role in myelinogenesis in developing brain. *EMBO J.* (2017) doi:10.15252/embj.201696056.

33. Reichert, F. & Rotshenker, S. Galectin-3 (MAC-2) controls microglia phenotype whether amoeboid and phagocytic or branched and non-phagocytic by regulating the cytoskeleton. *Front. Cell. Neurosci.* (2019) doi:10.3389/fncel.2019.00090.

34. Bialas, A. R. *et al.* Microglia-dependent synapse loss in type i interferon-mediated lupus. *Nature* (2017) doi:10.1038/nature22821.

35. Liu, C. C. *et al.* Interferon alpha inhibits spinal cord synaptic and nociceptive transmission via neuronal-glial interactions. *Sci. Rep.* (2016) doi:10.1038/srep34356.

36. Butler, A., Hoffman, P., Smibert, P., Papalexi, E. & Satija, R. Integrating single-cell transcriptomic data across different conditions, technologies, and species. *Nat. Biotechnol.* (2018) doi:10.1038/nbt.4096.

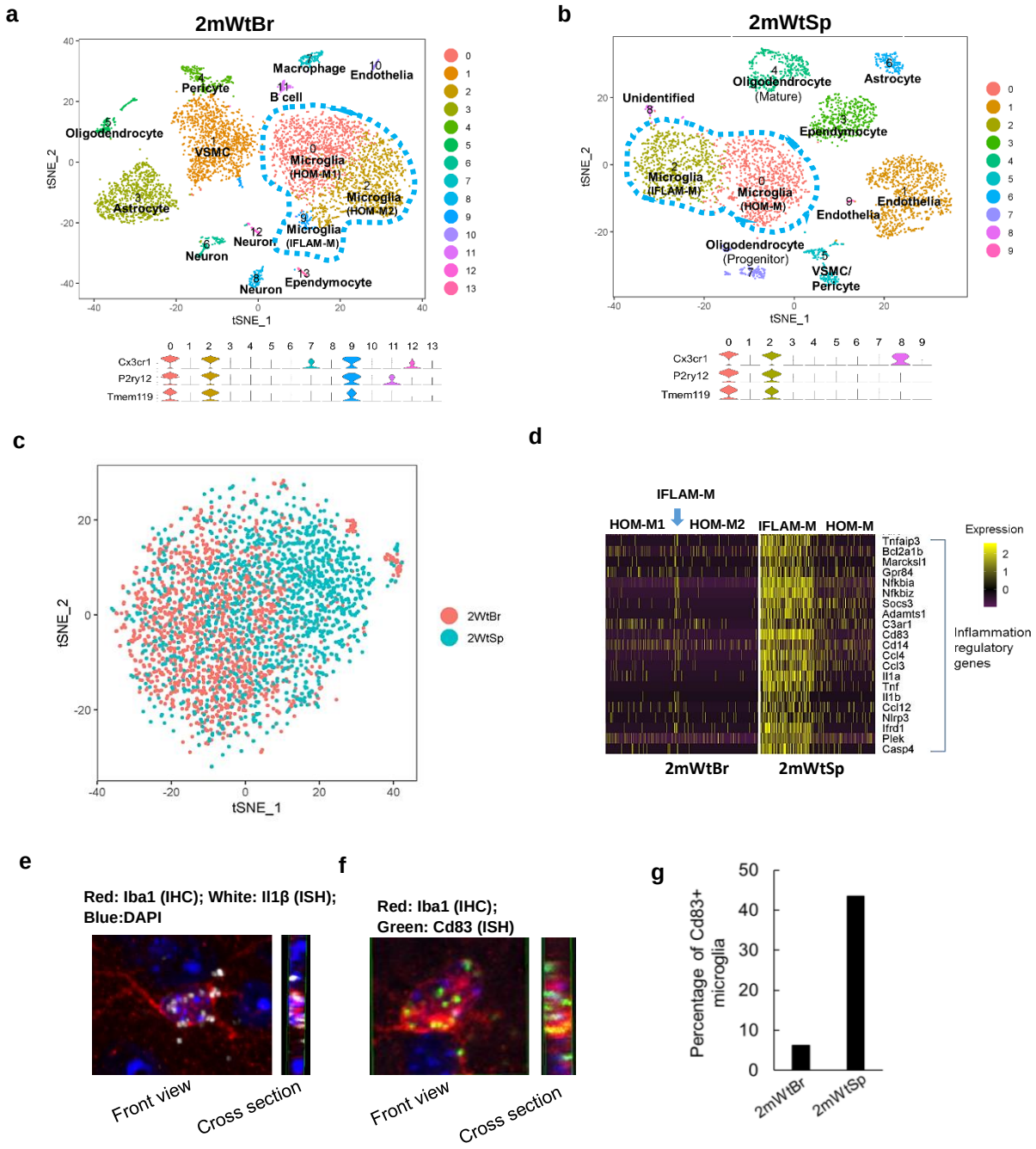

Figure 1. **Single cell RNA-seq (scRNA-seq) analysis revealed region-specific microglial subtypes from the 2-month wild type (Wt) brain cortex (2mWtBr) and spinal cord (2mWtSp).** **a** and **b.** t-SNE plot identified microglial clusters (blue dot line circled) from cells dissociated from the 2mWtBr (**a**) and 2mWtSp (**b**) respectively. Based on the expressed signature genes, these microglia were characterized as homeostatic microglia (HOM-M) and proinflammatory microglia (IFLAM-M). Cortical HOM-M were further separated into HOM-M1 an HOM-M2. Violin plots (the lower panels) demonstrated the expression of microglial marker genes Cx3cr1, P2ry12, and Tmem119 in the corresponding clusters. **c** Seurat Canonical Correlation Analysis (CCA) analysis demonstrated that spinal microglia were partially overlapped with cortical microglial cluster which indicated microglia region-dependent heterogeneity. **d.** Gene expression heatmap demonstrated a high population of inflammatory microglia in spinal cord but low in the brain cortex. Each row represents a gene and each column represents a cell. **e**. Z-stack image of the combined immunohistochemistry (IHC) and RNAscope in situ hybridization (ISH) demonstrated the expression of Il1b in the cortical microglia. **f.** Z-stack image of the combined IHC and ISH demonstrated the expression of Cd83 in the spinal microglia. **g**.The percentage of $Cd83^{+}Iba1^{+}$ microglia in the 2-month Wt brain cortex and spinal cord.

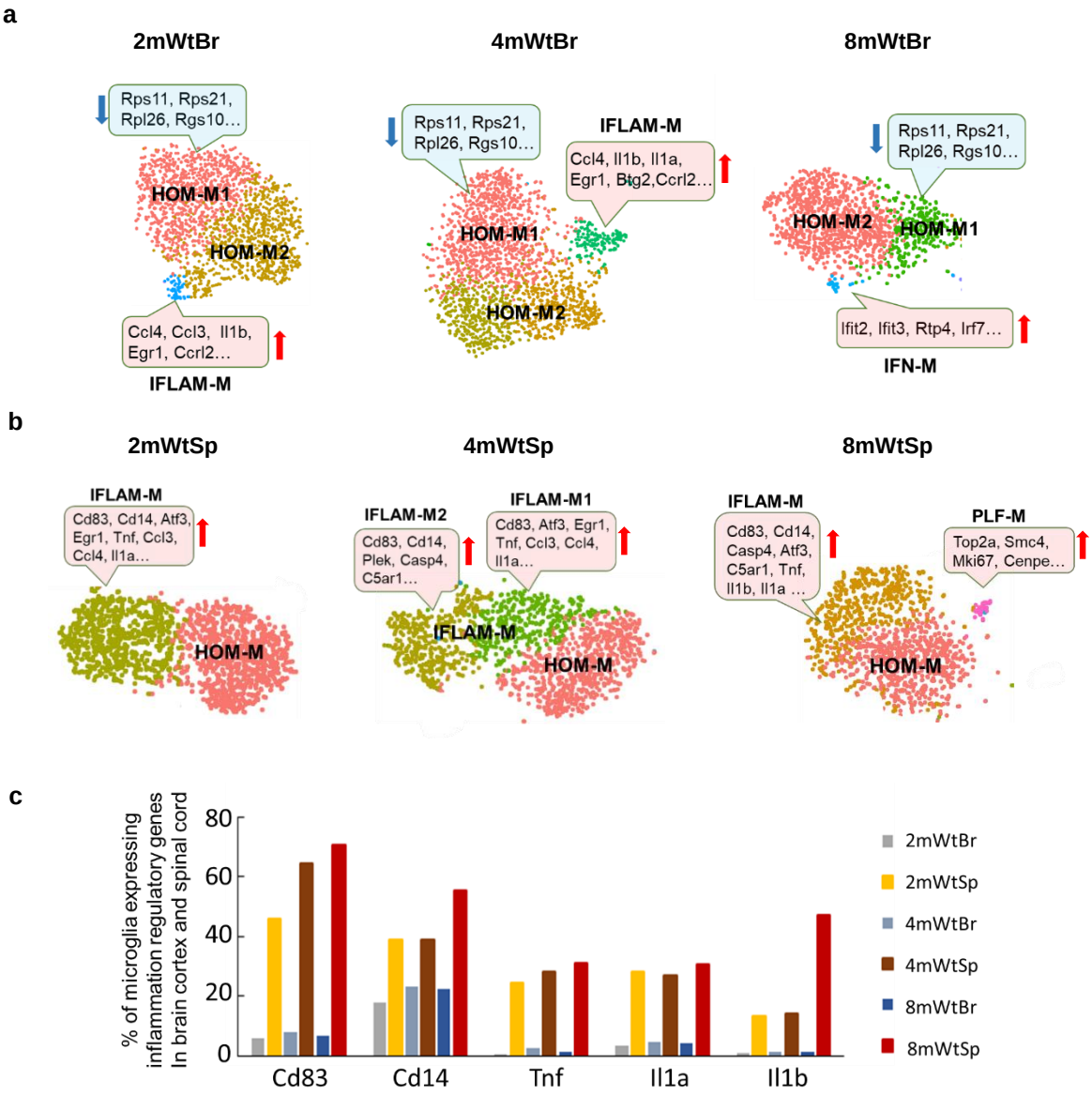

Figure 2. **Cortical and spinal microglia temporal changes in the 2-, 4-, and 8-month Wt mice. a.** The temporal change of cortical microglia in the 2-, 4-, and 8-month cortex**.** HOM-M were polarized into HOM-M1 and HOM-M2 at all ages with HOM-M1 expressed lower level of genes including Rps11, Rps21, Rpl26, Rgs10 (blue highlighted). IFLAM-M constituted a small percentage of cortical microglia in the 2- and 4-month. At the 8-month, IFLAM-M was not observed. Instead a small population of interferon related microglia (IFN-M) was appeared. The pink highlighted are the highly expressed genes in the corresponding clusters. **b**. The temporal change of IFLAM-M in the 2-, 4- and 8-month Wt spinal cord. The IFLAM-M were separated into two different clusters IFLAM-M1 and IFLAM-M2 at 4-month with their distinct set of upregulated genes (pink highlighted). At 8month, a small microglial cluster expressing genes regulating cell cycle and proliferation (PLF-M) was observed in the 8-month Wt spinal cord. **c.** The increased number of microglia expressing inflammation related genes in the 8-month Wt spinal cord but not cortex.

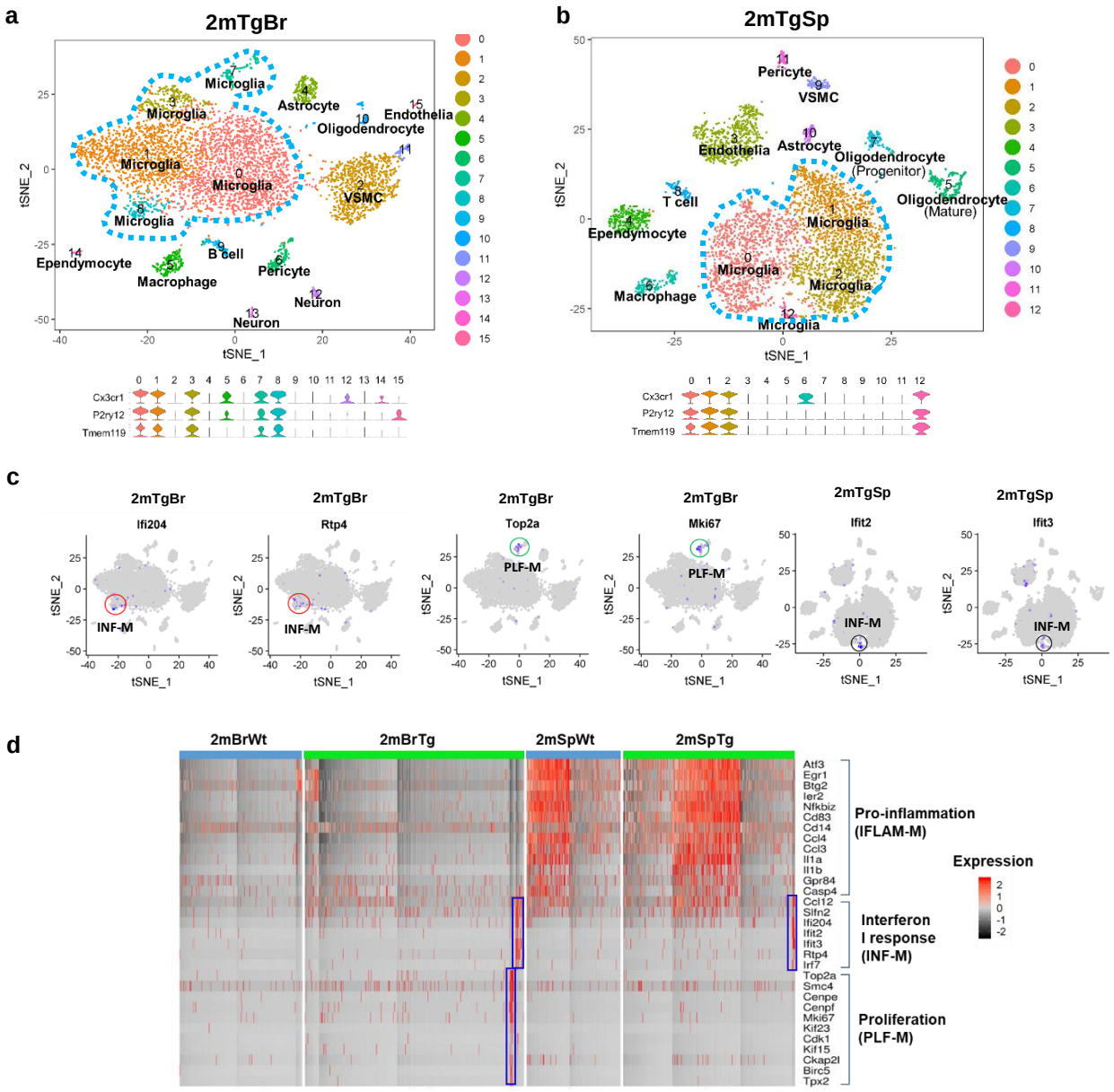

Figure 3. HIV-gp120 induced region-specific microglia heterogeneity in the 2-month transgenic (Tg) brain cortex (2mTgBr) and spinal cord (2mTgSp). a and **b**. t-SNE identified five cortical and four spinal microglial clusters (blue dot line circled) from the 2-month Tg cortex (2mTgBr) and spinal cord (2mTgSp) respectively. **c.** Feature plots demonstrated the cluster of INF-M (red circled) and PLF-M (blue circled) in the 2-month Tg cortex and INF-M (black circled) in the 2-month Tg spinal cord respectively. **d**. Heatmap revealed the gp120 induced INF-M and PLF-M in the cortex but only the INF-M in the spinal cord.

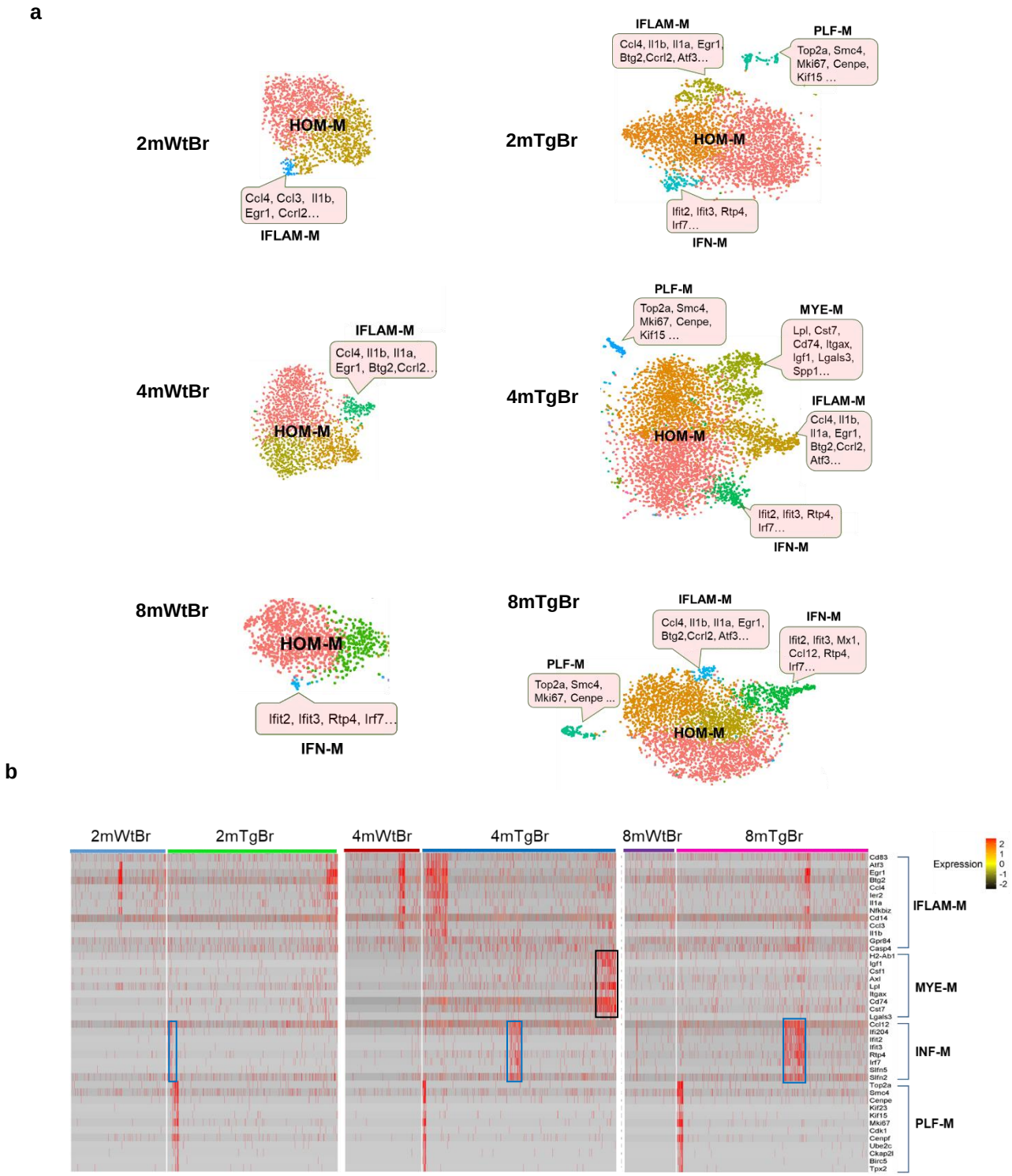

Figure 4. gp120 temporally promoted cortical microglial heterogeneity in the Tg mice. a. tSNE plots demonstrated gp120 increased microglia heterogeneity in 2-, 4-, and 8-month Tg brain cortices. Gp120 induced INF-M and PLF-M at all ages in the cortices. Microglia expressed gene mediating demyelination and re-myelination (MYE-M) was only induced in the 4month Tg brain cortex (4mTgBr). The pink highlighted are the enriched expressed genes in the corresponding clusters **b**. Heat map demonstrated the expression of feature genes of IFLAM-M, MYE-M, INF-M and PLF-M respectively. Notice the MYE-M (black rectangle) was only showed in the 4-month Tg cortices. INF-microglia (blue rectangle) were gradually increased with aging in the Tg cortices.

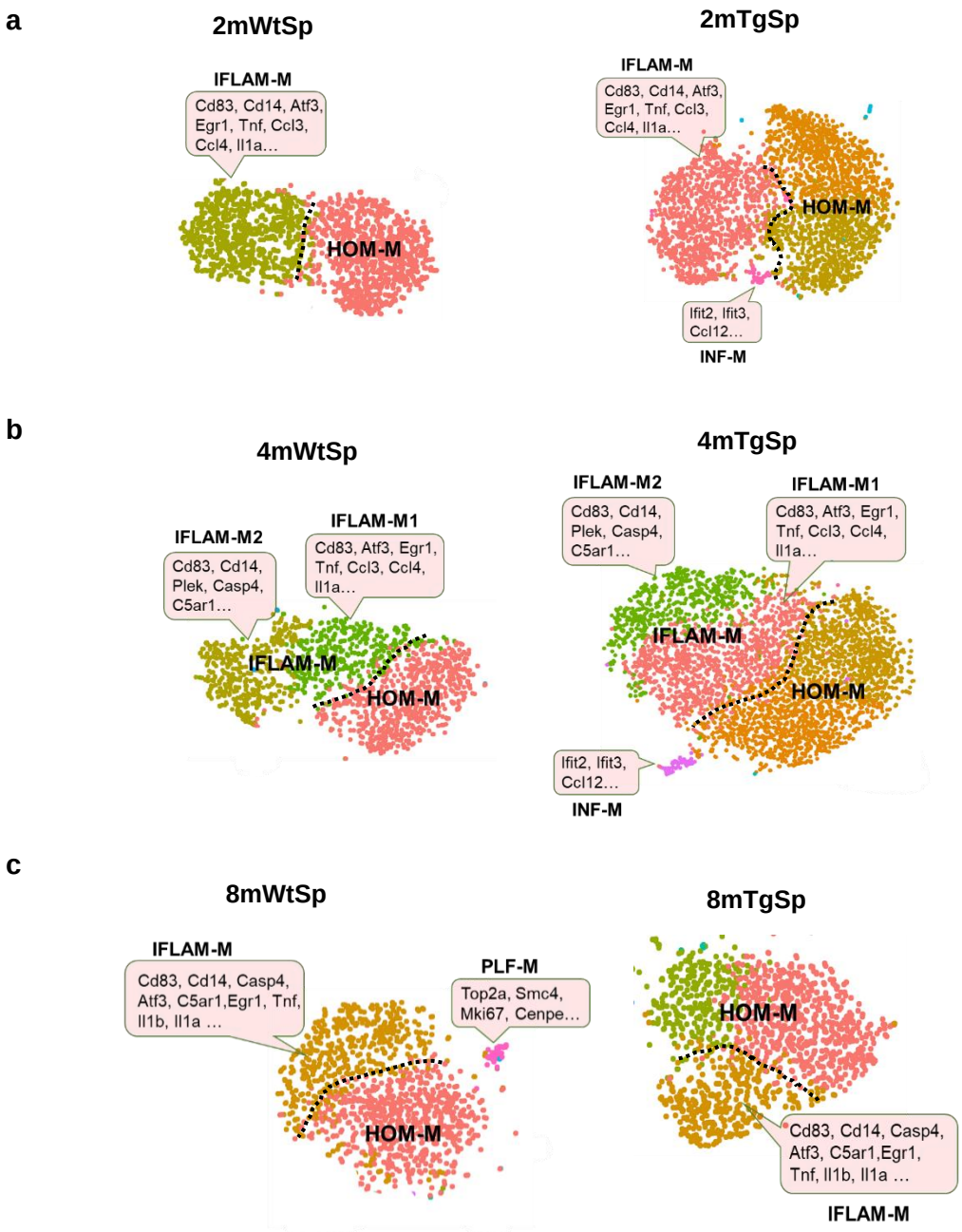

Figure 5. gp120 temporally changed the spinal microglial heterogeneity in the Tg mice. Contrast to the wild type counterparts, gp120 induced INF-M in the 2- (**a**) and 4-month Tg spinal cord (**b**). gp120 did not increase microglia heterogeneity in the spinal cord at 8-month (**c**). Instead, the PLF-M detected at 8-month Wt spinal were not detected in the 8-month Tg spinal cord. Dot line separated the HOM-M with the IFLAM-M. The pink highlighted are the enriched expressed genes in the corresponding clusters.

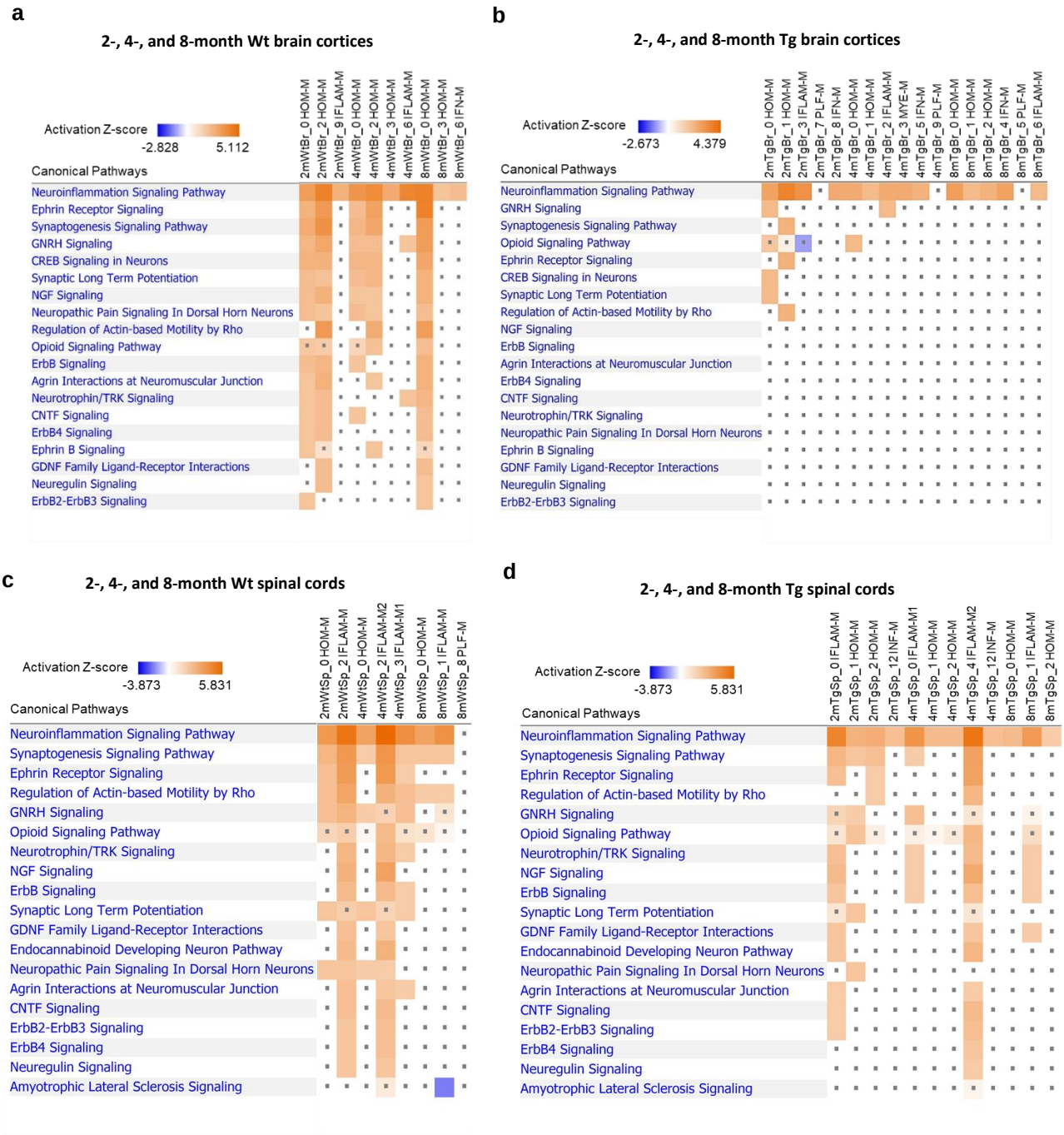

Figure 6. **The effect of HIV-1 gp120 on cortical and spinal microglial nervous signaling pathways**. **a**. Ingenuity Pathway Analysis (IPA) predicted the activated nervous signaling pathways of cortical microglia in the 2-, 4-, and 8-month Wt cortices. **b**. The activated cortical microglial signaling were severely suppressed by gp120 in the Tg brain cortices at all ages. **c**. IPA predicted the activated nervous signaling pathways of spinal microglia in the 2-, 4-, and 4-month Wt spinal cords. **d**.The activated nervous signaling of spinal microglia were differentially attenuated by gp120 in the Tg spinal cords. Note the signaling of IFLAM-M were attenuated in a less degree compared to spinal HOM-M and all the cortical microglia. Microglia were labeled as: Experimental group_ # of microglial cluster followed by name of microglial subtype. Orange: activated signaling. Blue: inhibited signaling. Dot: not significantly changed.

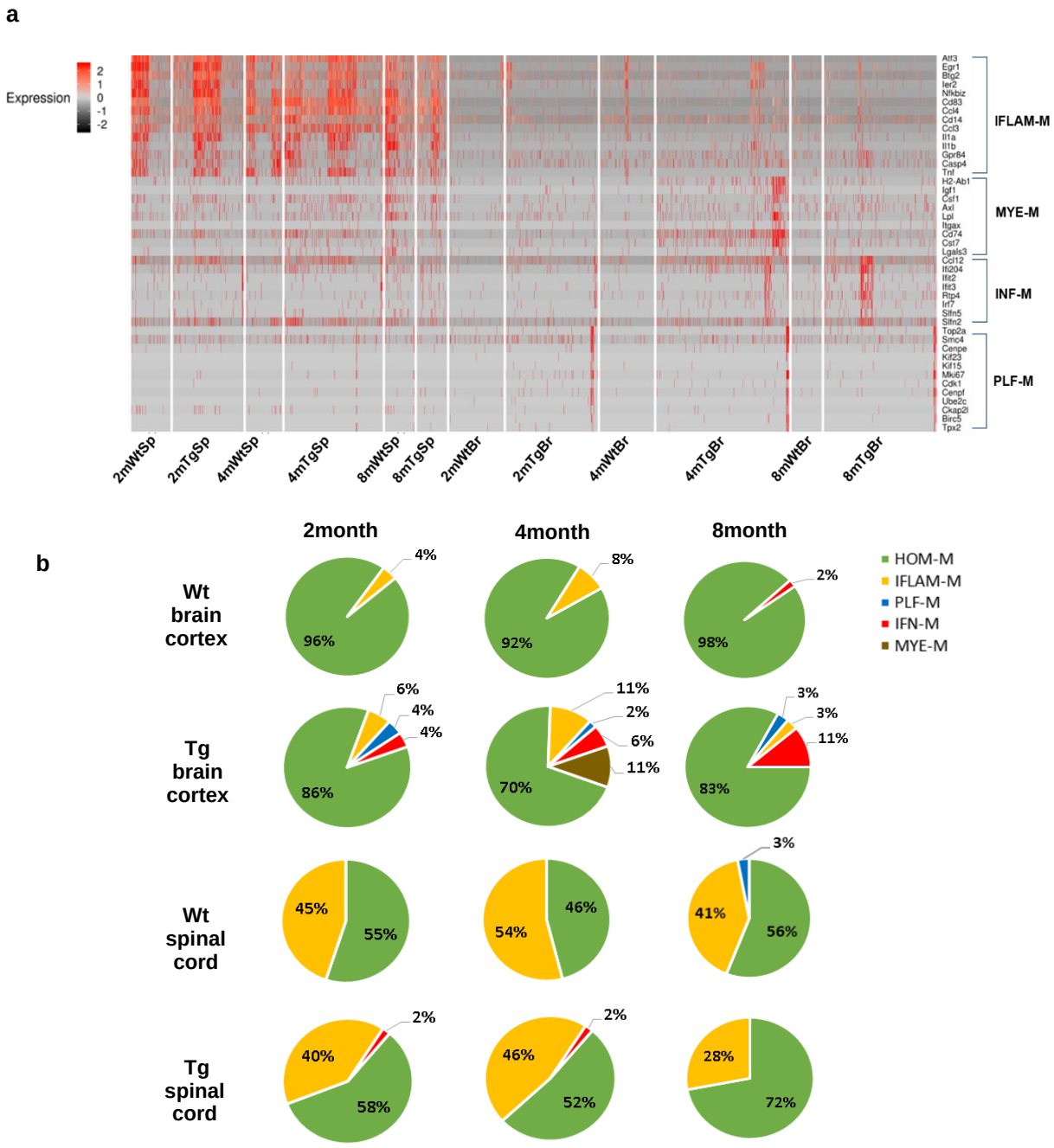

Figure 7. Microglia subtypes from the 2-, 4-, 8-month Wt and Tg cortices and spinal cords. **a.** The gene expression heatmap demonstrated highly expressed genes in different microglia subtypes in the Wt and Tg brain cortices and spinal cords. **b**. A pie chart showing the population sizes of microglia subtypes in the 2-, 4-, 8-month Wt and Tg cortices and spinal cords.

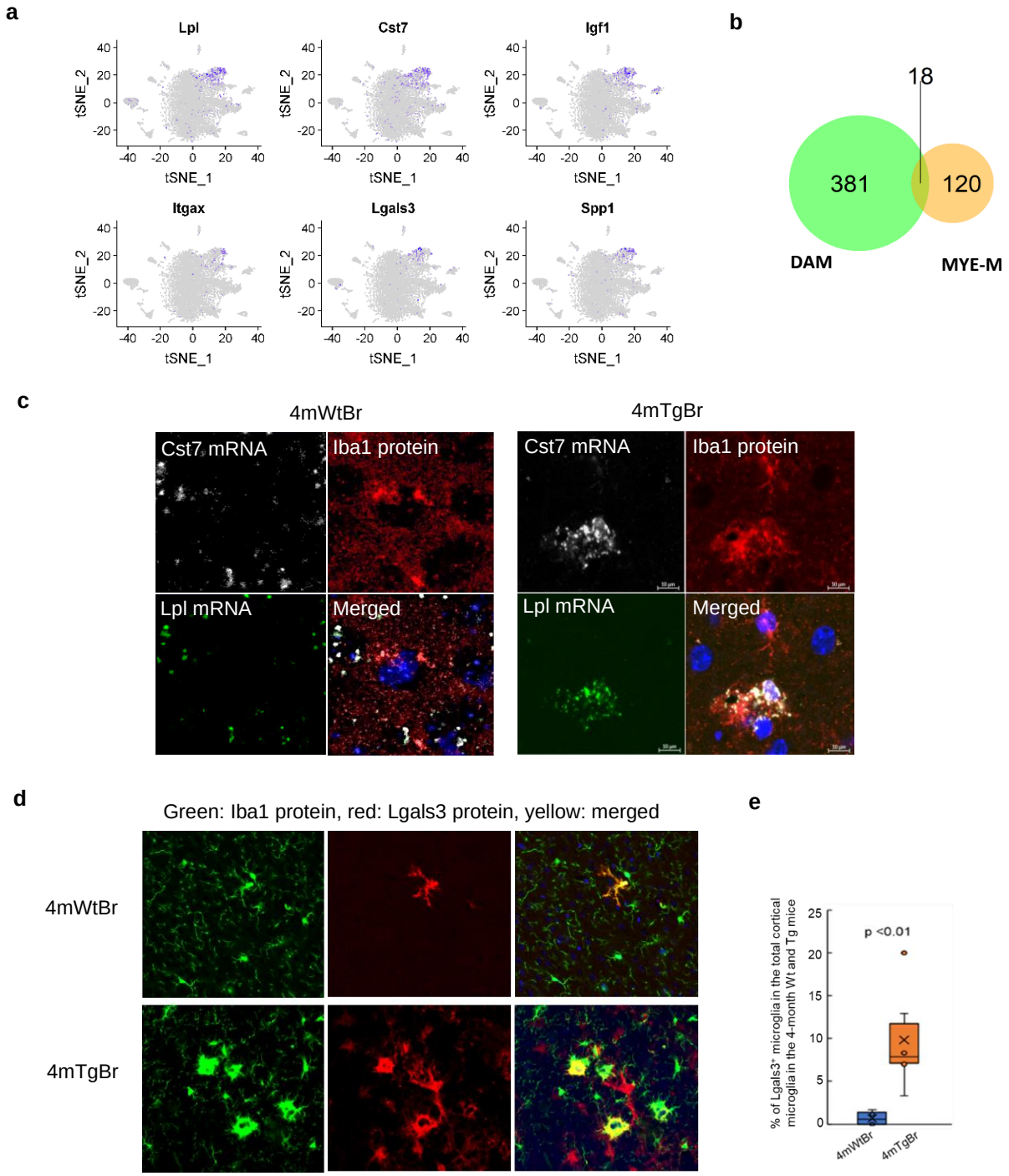

Figure 8. Verification of the MYE-M on tissue. a. Feature plots demonstrated the MYE-M uniquely expressed genes in the 4-month Tg brain cortex (4mTgBr). **b.** Venn diagram revealed 13% of the genes upregulated in the MYE-M were also upregulated in the disease associated microglia (DAM) identified in the Alzheimer's Disease mouse brain. **c**. RNAscope ISH combined with IHC demonstrated the high expression of Cst7 and Lpl mRNA in microglia in the 4-month Tg but very low in the Wt brain cortices. **d** and **e**. IHC showed the Lgals3^{+}Iba1^{+} microglia in the 4-month Wt and Tg cortices and their quantification (**e**). The percentage of Lgals3^{+}Iba1^{+} in the 4mTgBr and 4mWtBr.

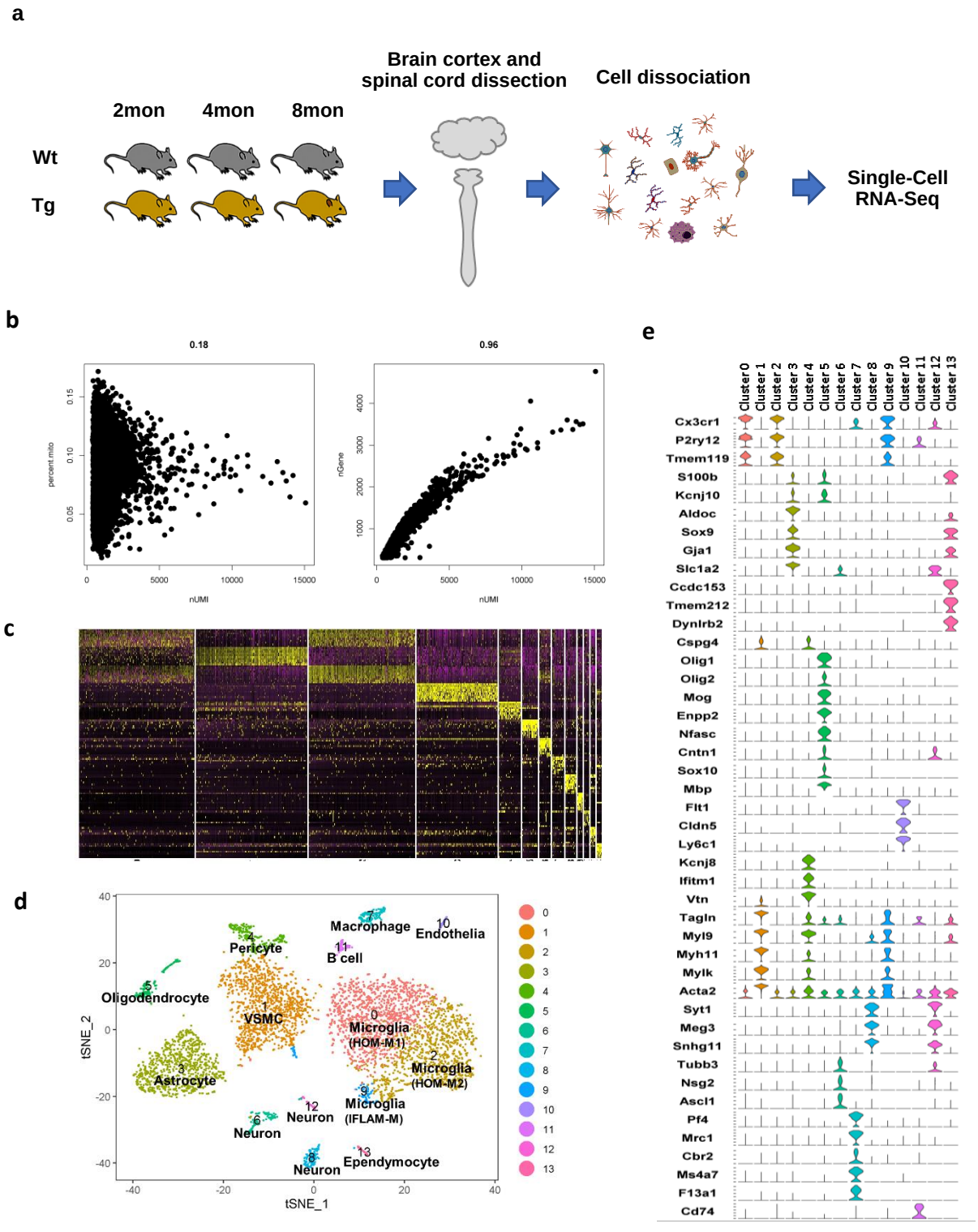

Supplementary Figure 1. Workflow of the single cell RNA-seq (scRNA-seq) experiment and data analysis for the 2-month Wt brain cortex. **a**: A diagram showing the workflow of cell dissociation and scRNA-seq**. b**: QC metrics showed the percentage of mitochondrial genes, and number of genes detected per cell. nUMI: number of unique molecular identifiers. **c**. Gene expression heatmap demonstrated the top 10 variable genes in each cluster. **d**. t-SNE plots displayed the well separated cell type of individual cluster. **e**: Combined Violent Plot demonstrated multiple gene markers for the cell type corresponding to the cluster number.

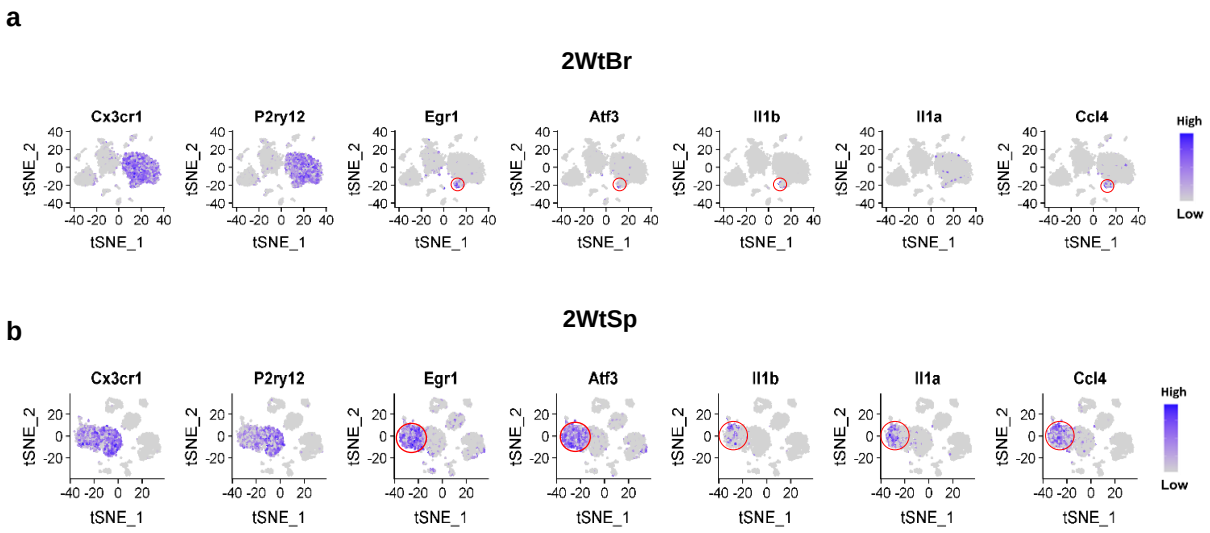

Supplementary Figure 2. Feature plots demonstrated the markedly different population of inflammatory microglia (IFLAM-M) in the 2-month Wt brain cortex (2mWtBr) and 2-month Wt spinal cord (2mWtSp). Feature plots of gene Cx3cr1, P2ry12 demonstrated all microglia population in the cortex (a) and spinal cord (b). Feature plots of IFLAM-M signature genes (Egr1, Atf3, Il1a, Il1b, Ccl4) showed the population of IFLAM-M (red circled) in the cortex (a) and spinal cord (b). Blue: high expression. Gray: low expression.

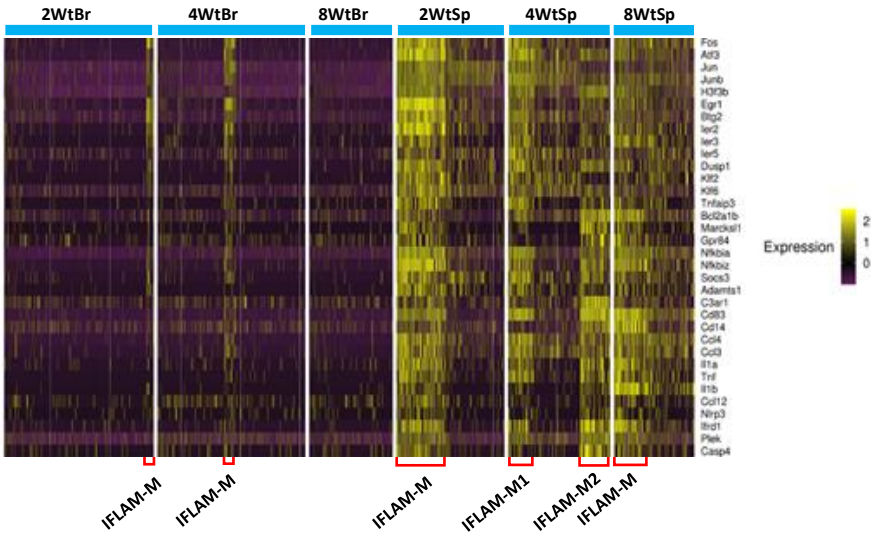

Supplementary Figure 3. Gene expression heatmap demonstrated the population of IFLAM-M (red bracket) in the 2-, 4- and 8-month Wt brain cortices and spinal cords.